

**AD-A279 408**



## Transient Photoluminescence Measurements on GaAs and AlGaAs Double Heterostructures

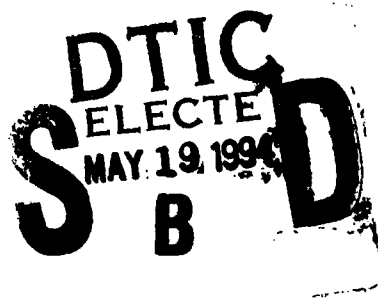
15 August 1993

Prepared by

L. F. HALLE, S. C. MOSS, and D. C. MARVIN  
Electronics Technology Center  
Technology Operations

Prepared for

SPACE AND MISSILE SYSTEMS CENTER  
AIR FORCE MATERIEL COMMAND  
2430 E. El Segundo Boulevard  
Los Angeles Air Force Base, CA 90245



Engineering and Technology Group

**94 5 18 031**

APPROVED FOR PUBLIC RELEASE;  
DISTRIBUTION UNLIMITED

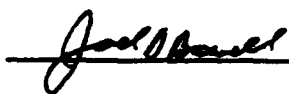
DTIC QUALITY INSPECTED 1

**Best  
Available  
Copy**

This report was submitted by The Aerospace Corporation, El Segundo, CA 90245-4691, under Contract No. F04701-88-C-0089 with the Space and Missile Systems Center, 2430 E. El Segundo Blvd., Los Angeles Air Force Base, CA 90245. It was reviewed and approved for The Aerospace Corporation by S. Feuerstein, Acting Principal Director, Electronics Technology Center. Lt. Joel Boswell was the project officer for the Mission-Oriented Investigation and Experimentation (MOIE) program.

This report has been reviewed by the Public Affairs Office (PAS) and is releasable to the National Technical Information Service (NTIS). At NTIS, it will be available to the general public, including foreign nationals.

This technical report has been reviewed and is approved for publication. Publication of this report does not constitute Air Force approval of the report's findings or conclusions. It is published only for the exchange and stimulation of ideas.

  
Joel Boswell, Lt. USAF  
SMC

  
Wm. Kyle Sneddon, Captain USAF  
Deputy, Industrial & International Division

REPORT DOCUMENTATION PAGE			Form Approved OMB No. 0704-0188	
Public reporting burden for this collection of information is estimated to average 1 hour per response, including the time for reviewing instructions, searching existing data sources, gathering and maintaining the data needed, and completing and reviewing the collection of information. Send comments regarding this burden estimate or any other aspect of this collection of information, including suggestions for reducing this burden to Washington Headquarters Services, Directorate for Information Operations and Reports, 1215 Jefferson Davis Highway, Suite 1204, Arlington, VA 22202-4302, and to the Office of Management and Budget, Paperwork Reduction Project (0704-0188), Washington, DC 20503.				
1. AGENCY USE ONLY (Leave blank)		2. REPORT DATE 15 August 1993		3. REPORT TYPE AND DATES COVERED
4. TITLE AND SUBTITLE Transient Photoluminescence Measurements on GaAs and AlGaAs Double Heterostructures			5. FUNDING NUMBERS  F04701-88-C-0089	
6. AUTHOR(S) Halle, Linda F.; Moss, Steven C.; and Marvin, Dean C.				
7. PERFORMING ORGANIZATION NAME(S) AND ADDRESS(ES) The Aerospace Corporation Technology Operations El Segundo, CA 90245-4691			8. PERFORMING ORGANIZATION REPORT NUMBER  TR-93(3925)-1	
9. SPONSORING/MONITORING AGENCY NAME(S) AND ADDRESS(ES) Space and Missile Systems Center Los Angeles Air Force Base Los Angeles, CA 90009-2960			10. SPONSORING/MONITORING AGENCY REPORT NUMBER  SMC-TR-94-26	
11. SUPPLEMENTARY NOTES				
12a. DISTRIBUTION/AVAILABILITY STATEMENT  Approved for public release; distribution unlimited			12b. DISTRIBUTION CODE	
13. ABSTRACT (Maximum 200 words)  We report a set of transient photoluminescence (TPL) measurements of GaAs and AlGaAs double heterostructure (DH) materials as a function of temperature from 10K to 300K. We also report measurements of the time-integrated photoluminescence spectra of these samples. We observe, in both the spectra and the TPL measurements, evidence that the low-temperature photoluminescence kinetics are affected by additional paths for radiative decay that are not evident at room temperature, but have implications for material qualities measured at room temperature.				
14. SUBJECT TERMS  Transient photoluminescence, GaAs, AlGaAs, Solar cells			15. NUMBER OF PAGES 7	
			16. PRICE CODE	
17. SECURITY CLASSIFICATION OF REPORT UNCLASSIFIED	18. SECURITY CLASSIFICATION OF THIS PAGE UNCLASSIFIED	19. SECURITY CLASSIFICATION OF ABSTRACT UNCLASSIFIED	20. LIMITATION OF ABSTRACT	

## Contents

ABSTRACT.....	1
INTRODUCTION.....	1
EXPERIMENTAL DETAILS .....	1
RESULTS .....	2
CONCLUSIONS.....	5
ACKNOWLEDGMENT.....	5
REFERENCES.....	5

Accession For	
NTIS GRA&I	<input checked="" type="checkbox"/>
DTIC TAB *	<input type="checkbox"/>
Unannounced	<input type="checkbox"/>
Justification	
By _____	
Distribution/Avail:	
Availability Codes	
Dist	Avail and/or Special
A-1	

## Figures

1. Measured RT lifetimes of GaAs DHs samples S1 and S3 as a function of incident optical fluence.....	2
2. Room temperature TPL measurements of GaAs DHs .....	2
3. PL spectra of S1 for temperatures from 300K to 11K.....	3
4. PL spectra at 10K for S1, S2, and S3.....	3
5. TPL measurements of S1 for temperatures from 300K to 10K.....	3
6. TPL measurements associated with different peaks of S1 .....	4
7. RT TPL measurements on AlGaAs DHs.....	4
8. PL spectra of S7 for temperatures from 300K to 11K.....	4
9. PL spectra at 10K for samples S7, S8, and S9.....	4
10. TPL measurements of S7 for temperatures from 300K to 10K.....	5
11. TPL measurements associated with different peaks of sample S7.....	5

## Tables

1. Characteristics of GaAs and AlGaAs double heterostructures .....	1
2. Room-temperature lifetimes.....	2

## TRANSIENT PHOTOLUMINESCENCE MEASUREMENTS ON GaAs AND AlGaAs DOUBLE HETEROSTRUCTURES

Linda F. Halle, Steven C. Moss, and Dean C. Marvin  
Electronics Technology Center, The Aerospace Corporation  
P. O. Box 92957, Los Angeles, CA 90009-2957

### ABSTRACT

We report a set of transient photoluminescence (TPL) measurements of GaAs and AlGaAs double heterostructure (DH) materials as a function of temperature from 10K to 300K. We also report measurements of the time-integrated photoluminescence spectra of these samples. We observe, in both the spectra and the TPL measurements, evidence that the low-temperature photoluminescence kinetics are affected by additional paths for radiative decay that are not evident at room temperature, but have implications for material qualities measured at room temperature.

### INTRODUCTION

The efficiency of solar cells is directly related to the carrier lifetimes of the materials forming the active regions of the cells, such as the GaAs or AlGaAs materials studied here. A standard method for measuring the carrier lifetimes is a technique known as transient photoluminescence [1]. We have extended this technique to studies as a function of temperature over the range of 10K to 300K. We have also measured time-integrated photoluminescence spectra. At high temperatures, we observe the broad, highly asymmetric band-to-band luminescence characteristic of these materials. At low temperatures (10K-25K), the spectral scans of both the GaAs and AlGaAs samples show two peaks. At low temperatures, we also performed wavelength-dependent TPL measurements. These spectrally dependent TPL measurements allow us to deduce the existence of unanticipated acceptor levels, incorporated during fabrication, that alter the photoluminescence spectra and TPL measurements at low temperature. The presence of these acceptor levels may affect the carrier mobility in this material, even at room temperature, depending on their density. Information regarding the density of these acceptor levels may be obtained from these types of measurements.

Transient photoluminescence measurements use picosecond laser pulses to excite a sample, and the luminescence from the sample is measured using a form of time-correlated, single-photon counting [2]. In DH materials, the picosecond laser pulse is absorbed near the front surface of the active layer. The charge carriers (electrons and holes) produced diffuse into the active layer and recombine through various mechanisms, some radiative and some non-radiative. The radiative recombination, measured in the form of luminescence, is a measure of the effective carrier lifetime. We have recently shown that this effective lifetime is, in general,

not the minority carrier lifetime [3]. Furthermore, the minority carrier lifetime can only be extracted from measurements of this type under carefully controlled experimental conditions [3].

### EXPERIMENTAL DETAILS

The sample characteristics are listed in Table 1. These samples were fabricated by Spire Corp. The substrates were semi-insulating GaAs. On top of this was grown a 1000Å GaAs buffer layer and a 1000Å barrier layer of  $\text{Al}_{0.8}\text{Ga}_{0.2}\text{As}$ . The n-type active regions were 2  $\mu\text{m}$  thick GaAs or  $\text{Al}_{0.1}\text{Ga}_{0.9}\text{As}$  doped with Se. The top layer was a 1000Å thick layer of  $\text{Al}_{0.8}\text{Ga}_{0.2}\text{As}$ . The energy bandgap of the barrier layers is large enough so that no laser light is absorbed in them. The active region is thick enough so that essentially all of the laser light is absorbed within the active region. The laser system consists of a cavity-dumped mode-locked dye laser synchronously pumped by the frequency-doubled output of an actively mode-locked Nd:YAG laser. We used a cavity dumping rate of 400 kHz, which ensured that the 2.5  $\mu\text{s}$  between pulses was much longer than the effective carrier lifetimes. The dye laser wavelength was 590 nm. The average dye laser power at this cavity dumping rate was 6 mW attenuated to 0.01 mW incident upon the sample. The laser pulses were 20 ps in duration (FWHM of intensity), were polarized, and were incident upon the samples at an angle of 27 degrees from normal. The laser pulse spot size on the sample was elliptical with the major axis being 5.7 mm (FW1/eM of intensity) and the minor axis being 4.8 mm (FW1/eM of intensity). The sample was enclosed in a temperature-controlled cryostat that allowed access to sample temperatures from 10K to 300K (RT).

Table 1. Characteristics of GaAs and AlGaAs double heterostructures.

Sample #	Type of Active Layer	Thickness of Active Layer ( $\mu\text{m}$ )	Active Layer Dopant Density ( $\text{cm}^{-3}$ )
S1	GaAs	2	$3.5 \times 10^{16}$
S2	GaAs	2	$9.0 \times 10^{16}$
S3	GaAs	2	$1.3 \times 10^{18}$
S7	$\text{Al}_{0.1}\text{Ga}_{0.9}\text{As}$	2	$3.5 \times 10^{16}$
S8	$\text{Al}_{0.1}\text{Ga}_{0.9}\text{As}$	2	$9.0 \times 10^{16}$
S9	$\text{Al}_{0.1}\text{Ga}_{0.9}\text{As}$	2	$1.3 \times 10^{18}$

We performed two kinds of measurements. One set of measurements consisted of the regular TPL measurements described above. The other set of measurements consisted of measurements of time-integrated photoluminescence spectra obtained by scanning the monochromator through various spectral regions during picosecond laser excitation of the sample. All of these measurements were performed in the room-temperature, low-intensity limit, where the decay of the band-to-band luminescence was independent of excitation intensity [3]. Of course, as the sample temperature decreases, so does the number of ionized donors,  $N_D$ . Consequently, it may not be possible to perform TPL measurements in the low-intensity limit for all sample temperatures.

## RESULTS

In order to obtain an accurate minority carrier lifetime measurement from the TPL technique, the excitation intensity must be such that the excited carrier concentration is much less than the donor concentration multiplied by the ratio of minority to majority carrier lifetimes [1]. The observed effective lifetimes as a function of intensity, measured at room temperature, for samples S1 and S3 are shown in Figure 1. The low-intensity lifetime is reached for these GaAs samples at fluences less than  $0.1 \text{ nJ/cm}^2$ . Similarly, the low-intensity limits are reached for the AlGaAs samples at fluences less than  $1 \text{ nJ/cm}^2$ . For the spectral scans and TPL measurements described below, the excitation fluence used was approximately  $0.1 \text{ nJ/cm}^2$ . In the GaAs and AlGaAs DHs, this resulted in a peak photogenerated carrier density of less than  $1 \times 10^{13}/\text{cm}^3$ . Since this is more than three orders of magnitude smaller than  $N_D$ , it indicates that the majority carrier lifetime is much greater than the minority carrier lifetime. These photogenerated carrier densities are small enough to avoid the exciton screening and renormalization effects observed in other picosecond measurements [4].

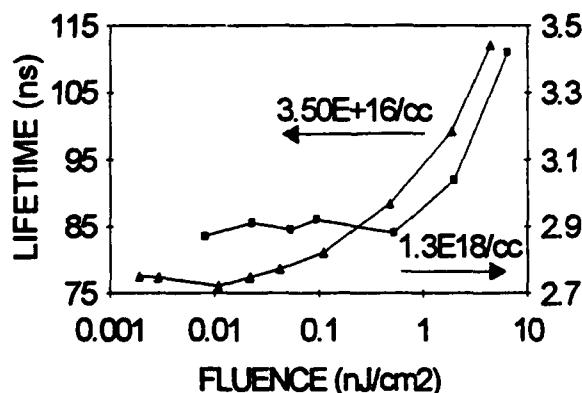


Figure 1. Measured RT lifetimes of GaAs DHs samples S1 and S3 as a function of incident optical fluence. Lifetimes(ns) for S3 correspond to scale at right.

### GaAs Double Heterostructures

TPL measurements at room temperature are shown for samples S1, S2, and S3 in Figure 2. The photolumines-

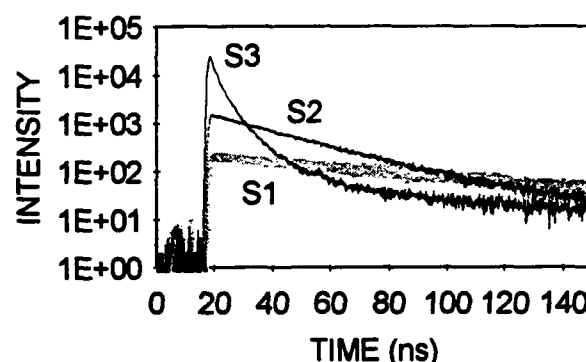


Figure 2. Room temperature TPL measurements of GaAs DHs.

cence rises rapidly during the absorption of the excitation pulse from a background level and then decays back to the background level with a lifetime that is characteristic of the properties of the sample. Single exponential fits to these decays indicate initial effective lifetimes of approximately 84, 30, and 3 ns for these samples, as listed in Table 2. The lifetimes expected due to band-to-band radiative recombination are 143, 56, and 4 ns, respectively. If we neglect surface recombination and Auger recombination, the minority lifetime can be extracted from these measurements taken in the low-intensity limit by using the equation  $1/\tau_{\text{eff}} = 1/\tau_{\text{BB}} + 1/\tau_p$ , where  $\tau_{\text{BB}} = 1/BN_D$  is the band-to-band radiative lifetime ( $B = 2 \times 10^{-10} \text{ cm}^6/\text{s}$ ) and where  $\tau_p$  is the minority carrier lifetime. These results place lower limits on the minority carrier lifetimes in samples S1, S2, and S3 of approximately 205 ns, 67 ns, and 11 ns, respectively. Note that S3 has different decay rates at longer times, which may be due to the effects of photon recycling or of de-trapping phenomena, or could be due to the effects of multiple recombination centers or recombination at dislocation sites. Similar effects are observed in the room-temperature TPL measurements on the AlGaAs samples.

Table 2. Room-temperature lifetimes.

Sample #	Measured RT Lifetime (nsec)	B-B Lifetime (nsec)	Estimated Lower Limits of $\tau_p$ (nsec)
S1	84.2	143	205
S2	30.4	55.6	67.1
S3	2.85	3.8	11.4
S7	63.6	143	114.5
S8	14.5	55.6	19.6
S9	< 0.8	3.8	< 1.0

An example of a set of spectral scans for sample S1, a GaAs DH, is shown in Figure 3. At low temperatures, the spectrum shows two peaks centered at 8185 and 8295 Å, corresponding to 1.515 eV and 1.495 eV. In all of these measurements, the results are a convolution of the instrument response function with the actual spectrum. The spectral resolution ranged from 10-15 Å at low temperatures to approximately 50 Å at room temperature. The higher-energy



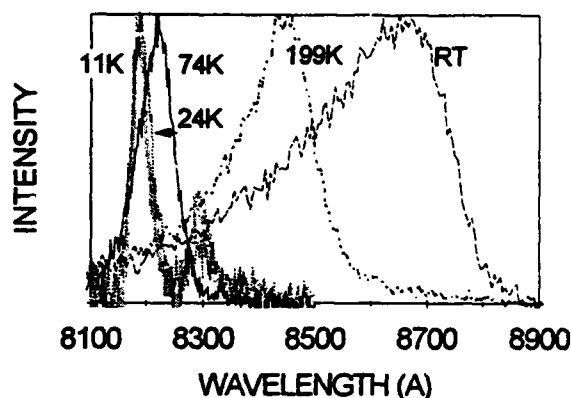


Figure 3. PL spectra of S1 for temperatures from 300K to 11K. Light gray curve is 11K spectrum, while the dotted curve is the 24K spectrum.

peak corresponds to the combined, spectrally unresolved effects of free-carrier (band-to-band), free-exciton, and bound-exciton luminescence from the sample [5]. The peak 20 meV below the bandgap corresponds to the combined, spectrally unresolved effects of luminescence due to conduction band-to-acceptor transitions and to donor-to-acceptor transitions [6]. The relative amplitudes of the two peaks at two different incident optical intensities are approximately equal. By 50K (not shown in the figure), the lower-energy transition has essentially disappeared. This temperature seems too low to cause a band-to-acceptor transition to disappear because  $k_B T$  (0.004 meV) is only one-fifth of the energy separation from the band. However, if the transitions were from the Se donor level (6 meV below the conduction band [7]) to a shallow acceptor level (14 meV above the valence band), the transition could be extinguished at 50K because most of the donors would be ionized. We also note that, as expected, the luminescence peaks shown in Figure 3 shift to longer wavelengths at higher temperatures. Furthermore, the peaks broaden substantially and become highly asymmetric at higher temperatures, as expected for band-to-band transitions. Similar spectra were seen for the GaAs samples S2 and S3 at the higher temperatures. At 11K and 24K, the two transitions are also seen in S2, but not in S3, as shown in Figure 4. The peaks for sample S2 are shifted by 1.8 meV to higher energies relative to sample S1. This is characteristic of samples in which conduction band-to-acceptor or donor-to-acceptor transitions occur. The broad unresolved low-temperature spectrum of sample S3 may indicate the combined effects of band-gap narrowing and broadening of the spectrum of donor and acceptor energy levels.

TPL measurements from 300K to 10K are shown in Figure 5. The effective lifetime decreases markedly with temperature. At room temperature, the effective lifetime is dominated by the band-to-band lifetime. As the temperature is lowered, the band-to-band lifetime increases due to the freezing out of carriers. However, the Shockley-Read-Hall lifetimes may decrease with temperature and have a larger effect on the effective lifetime at the intermediate temperatures. Surface recombination may play an important role in the TPL response. Its effects would be larger at lower temperatures due to the increasing value of the diffusion coefficient with declining temperature.

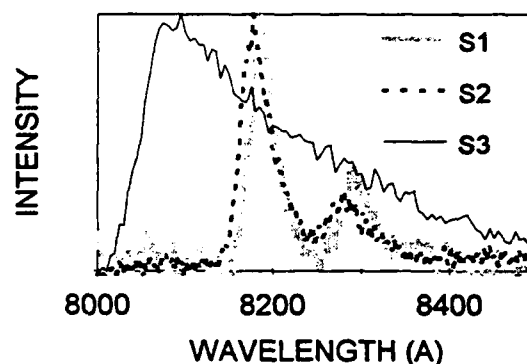


Figure 4. PL spectra at 10K for S1, S2, and S3.

We took TPL measurements of both peaks observed at the lowest temperatures. The TPL scan at 10K shown in Figure 5 is for the higher-energy peak seen in Figures 3 and 4. Figure 6 shows the TPL measurements on both of the low-temperature bands observed in sample S1. The TPL decay of the 1.515 eV luminescence is shown in curve (a). The initial decay is below the 1.2 ns resolution of our system. However, the TPL curve of the 1.495 eV luminescence, curve (b), decays with an initial time constant of approximately 20 ns. These recombination kinetics are consistent with a very fast relaxation of holes from the valence band down into the acceptor states, followed by a slower decay of the band-to-acceptor and/or donor-to-acceptor transition. The fast decay of the higher-energy peak also may include components due to the decay of free and bound excitons. Consequently, the decay of the initial excited carrier population at these low temperatures is dominated by the relaxation of holes into the acceptor levels and not by band-to-band or Shockley-Read-Hall recombination. At the elevated temperatures at which most solar cells are operated, it is unlikely that these processes will have a significant effect on solar cell efficiency. However, a high concentration of these defects can affect the room-temperature mobility of the material.

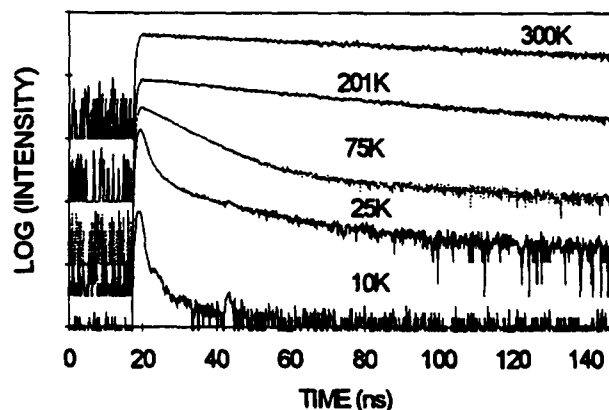


Figure 5. TPL measurements of S1 for temperatures from 300K to 10K. Calculated effective lifetimes are 84 ns (300K), 43 ns (201K), 7.9 ns (25K), and < 0.6 ns (10K).

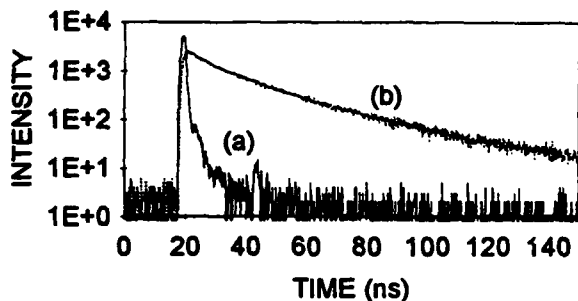


Figure 6. TPL measurements associated with different peaks of S1.

#### AlGaAs Double Heterostructures

TPL measurements at room temperature are shown for samples S7, S8, and S9 in Figure 7. Single exponential fits to these decays indicate initial effective lifetimes of approximately 64 and 14 ns for samples S7 and S8, respectively. The effective lifetime measured for S9 is less than 0.8 ns, smaller than the resolution of our experimental setup. The lifetimes for S7, S8, and S9 expected due to band-to-band radiative recombination are 143, 56, and 4 ns respectively, as listed in Table 2. Again, if surface recombination and Auger recombination are neglected, a lower limit to the minority lifetime can be extracted from these measurements taken in the low-intensity limit. These results

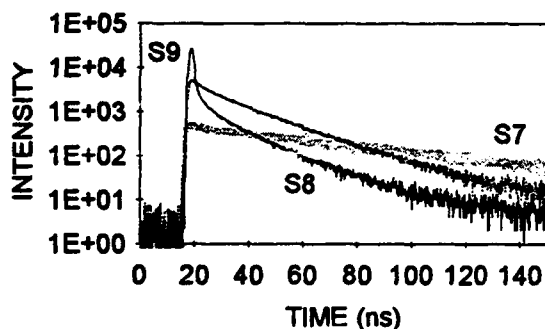


Figure 7. RT TPL measurements on AlGaAs DHs.

indicate that the minority carrier lifetimes in samples S7, S8, and S9 are approximately 114 ns, 20 ns, and < 1 ns, respectively. As with the highly doped GaAs sample S3, the highly doped AlGaAs sample has different decay rates at longer times, indicating the effects of other phenomena as discussed above.

An example of a set of spectral scans for sample S7, an AlGaAs DH, is shown in Figure 8. They show features similar to the spectral scans of the GaAs sample S1 shown in Figure 3. As with sample S1, at low temperatures, the spectrum shows two peaks, centered at 7534 Å and 7628 Å, corresponding to 1.645 eV and 1.625 eV. The identification of these two peaks is similar to that described above for the GaAs samples. Again, the relative amplitudes of the two peaks at two different incident optical intensities are approximately equal. The reasoning applied above to S1 also suggests that

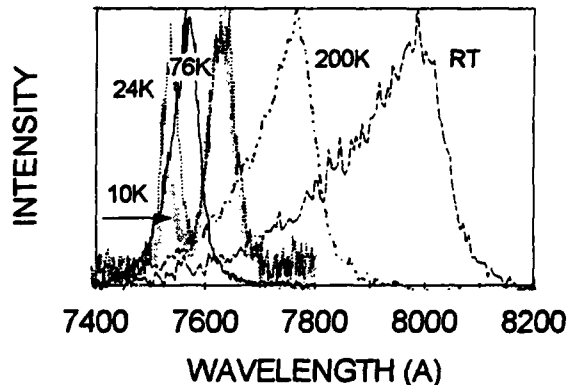


Figure 8. PL spectra of S7 for temperatures from 300K to 11K. Light gray curve is 11K spectrum, while the dotted curve is the 24K spectrum.

this transition in S7 is one from the Se donor level (6 meV below the conduction band [4]) to a shallow acceptor level (14 meV above the valence band). This would imply that the transition could be extinguished at 50K, as is observed, because most of the donors would be ionized. At 11K and 24K, two transitions are also seen in S8, but not in S9, as shown in Figure 9. The relative intensity of the lower-energy peak to the higher-energy peak is opposite that in the GaAs sample, perhaps indicating a higher density of these acceptor states. Again, as with the GaAs samples, the peaks of S8 are shifted to higher energy by approximately 1.8 meV. Sample S9 shows the same broadening effects as does sample S3.

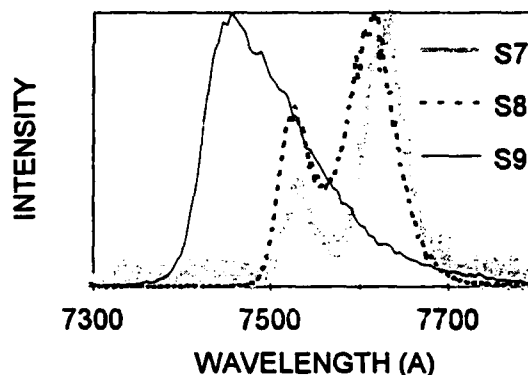


Figure 9. PL spectra at 10K for samples S7, S8, and S9.

TPL measurements from 300K to 10K for sample S7 are shown in Figure 10. As with the GaAs sample S1, the effective lifetime decreases with temperature for reasons discussed above. The TPL scan at 10K shown in Figure 10 is for the higher-energy peak seen in Figures 8 and 9. Figure 11 shows the TPL measurements on both of the low-temperature bands observed in sample S7. The decay of the 1.645 eV luminescence is shown in curve (a). The initial decay is below the 1.2 ns resolution of our system. The 1.625 eV luminescence, curve (b), decays with an initial time constant of approximately 23 ns and a longer decay constant at longer times. These recombination kinetics are similar to those described above for the GaAs samples.

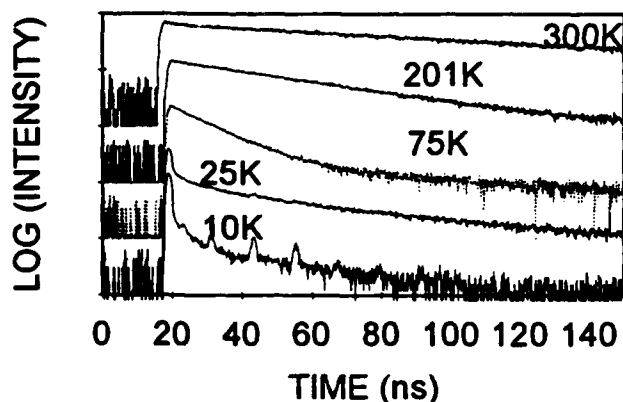


Figure 10. TPL measurements of S7 for temperatures from 300K to 10K. Calculated effective lifetimes are 64 ns (300K), 26 ns (201K), and < 1 ns (25K and 10K).

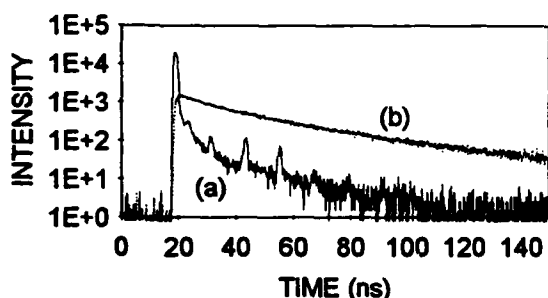


Figure 11. TPL measurements associated with different peaks of sample S7.

### CONCLUSIONS

We have performed a study of the photoresponse of GaAs and AlGaAs double heterostructures as a function of temperature from 300K to 10K. Additional paths for radiative recombination are observed at low temperatures that are not apparent at room temperature. We attribute the low-temperature results to a combination of band-to-band free-carrier recombination, free- and bound-exciton recombination, conduction band-to-acceptor recombination, and donor-to-

acceptor recombination. While the existence of these acceptor levels may not be apparent from TPL measurements performed at room temperature, their presence may affect room-temperature carrier lifetimes and carrier mobilities and, thus, solar cell performance.

This work demonstrates the extension of the TPL method into low-temperature, transition-specific studies. TPL appears to have the potential to characterize defect levels and concentrations in bulk materials, information which presently is obtained by deep-level transient spectroscopy on device structures. Information on the defects present in materials grown at different temperatures and with different MOCVD precursors is essential for the selection of the optimum growth methods for high-efficiency solar cell materials.

Additional measurements on samples with different active-layer thicknesses are in progress in order to quantify the surface recombination effects. Changes in the experimental apparatus are under way that will allow us to improve both the spectral and temporal resolution of our measurements. These changes may allow us to identify the impurities and make estimates of their densities.

### ACKNOWLEDGMENT

The authors gratefully acknowledge the support and encouragement of L. H. Thaller and J. A. Gelbwachs. This research was supported by the U. S. Air Force Space and Missiles Center under contract #F04701-88-C-0089.

### REFERENCES

1. D. C. Marvin and L. F. Halle, *21st IEEE PVSC*, 1990, p. 353.
2. D. V. O'Connor and D. Phillips, *Time-Correlated Single Photon Counting* (Academic, New York), 1984.
3. D. C. Marvin, S. C. Moss, and L. F. Halle, *J. Appl. Phys.* **72**, 1992, p. 1970.
4. C. V. Shank, R. L. Fork, R. F. Leheny, and J. Shah, *Phys. Rev. Lett.* **42**, 1979, p. 112.
5. M. L. W. Thawalt, M. Nissen, D. J. S. Beckett, and S. Charbonneau, *Inst. Phys. Conf. Ser. No. 95* (IOP, London), 1988, p. 505.
6. D. Bimberg, H. Munzel, A. Steckenborn, and J. Christen, *Phys. Rev. B* **31**, 1985, p. 7788.
7. S. M. Sze, *Physics of Semiconductor Devices* (John Wiley & Sons, New York), 1981.

## TECHNOLOGY OPERATIONS

The Aerospace Corporation functions as an "architect-engineer" for national security programs, specializing in advanced military space systems. The Corporation's Technology Operations supports the effective and timely development and operation of national security systems through scientific research and the application of advanced technology. Vital to the success of the Corporation is the technical staff's wide-ranging expertise and its ability to stay abreast of new technological developments and program support issues associated with rapidly evolving space systems. Contributing capabilities are provided by these individual Technology Centers:

**Electronics Technology Center:** Microelectronics, solid-state device physics, VLSI reliability, compound semiconductors, radiation hardening, data storage technologies, infrared detector devices and testing; electro-optics, quantum electronics, solid-state lasers, optical propagation and communications; cw and pulsed chemical laser development, optical resonators, beam control, atmospheric propagation, and laser effects and countermeasures; atomic frequency standards, applied laser spectroscopy, laser chemistry, laser optoelectronics, phase conjugation and coherent imaging, solar cell physics, battery electrochemistry, battery testing and evaluation.

**Mechanics and Materials Technology Center:** Evaluation and characterization of new materials: metals, alloys, ceramics, polymers and their composites, and new forms of carbon; development and analysis of thin films and deposition techniques; nondestructive evaluation, component failure analysis and reliability; fracture mechanics and stress corrosion; development and evaluation of hardened components; analysis and evaluation of materials at cryogenic and elevated temperatures; launch vehicle and reentry fluid mechanics, heat transfer and flight dynamics; chemical and electric propulsion; spacecraft structural mechanics, spacecraft survivability and vulnerability assessment; contamination, thermal and structural control; high temperature thermomechanics, gas kinetics and radiation; lubrication and surface phenomena.

**Space and Environment Technology Center:** Magnetospheric, auroral and cosmic ray physics, wave-particle interactions, magnetospheric plasma waves; atmospheric and ionospheric physics, density and composition of the upper atmosphere, remote sensing using atmospheric radiation; solar physics, infrared astronomy, infrared signature analysis; effects of solar activity, magnetic storms and nuclear explosions on the earth's atmosphere, ionosphere and magnetosphere; effects of electromagnetic and particulate radiations on space systems; space instrumentation; propellant chemistry, chemical dynamics, environmental chemistry, trace detection; atmospheric chemical reactions, atmospheric optics, light scattering, state-specific chemical reactions and radiative signatures of missile plumes, and sensor out-of-field-of-view rejection.